Available online at www.sciencedirect.com
SCIENCE DIRECT
Biochemical Pharmacology 68 (2004) 675–688
Biochemical Pharmacology
www.elsevier.com/locate/biochempharm

Agonist binding and activation of the rat β_1-adrenergic receptor: role of $Trp^{134\ (3.28)}$, $Ser^{190\ (4.57)}$ and $Tyr^{356\ (7.43)}$

Linda A. Rezmann-Vitti[a], Simon N.S. Louis[a], Tracy L. Nero[a], Graham P. Jackman[a], Dimitri Iakovidis[a], Curtis A. Machida[b], William J. Louis[a,*]

[a]*Department of Medicine, Clinical Pharmacology and Therapeutics Unit, The University of Melbourne, Austin Health, Heidelberg 3084, Vic., Australia*
[b]*Department of Integrative Biosciences, School of Dentistry, Oregon Health and Science University, Portland, OR 97239, USA*

Received 7 January 2004; accepted 27 April 2004

Abstract

We investigated the role of $Trp^{134\ (3.28)}$, $Ser^{190\ (4.57)}$ and $Tyr^{356\ (7.43)}$ in agonist binding to, and activation of, the rat β_1-adrenergic receptor by comparing pK_is and functional responses of W134A, S190A and Y356F mutant receptors to wild type, all stably expressed in CHO cells. All three mutations significantly ($P < 0.05$) reduced adenylyl cyclase intrinsic activity (IA) compared to wild type in response to stimulation with both (−)-isoprenaline (53–88%) and (−)-RO363 (46–61%), and there was no significant correlation either between IA or pD_2 and pK_i ($P > 0.4$), suggesting that changes in pK_i were not sufficient to explain the fall in adenylyl cyclase activity. The most pronounced reduction in affinity (126-fold, $P < 0.01$) was displayed by xamoterol for the Y356F mutation, suggesting that xamoterol is able to directly interact with $Tyr^{356\ (7.43)}$. For the other agonists, the change in pK_i values for the mutant receptors ranged from a 20-fold decrease to a 2-fold increase compared to the wild type. In a three-dimensional model of the rat β_1-adrenergic receptor, $Trp^{134\ (3.28)}$ and $Tyr^{356\ (7.43)}$ form part of a hydrophobic binding pocket involving residues in transmembrane helices 1, 2, 3 and 7. Our results suggest that $Trp^{134\ (3.28)}$ and $Tyr^{356\ (7.43)}$, together with $Trp^{353\ (7.40)}$, are able to interact via π–π interactions to stabilize the extracellular ends of transmembrane helices 3 and 7. $Ser^{190\ (4.57)}$ appears to be involved in a hydrogen bonding network, which maintains the spatial relationship between transmembrane helices 3 and 4. These interhelical interactions suggest that the three mutated residues stabilize the active receptor state by maintaining the proper packing of their respective transmembrane helix within the helix bundle, facilitating the appropriate movement and rotation of the transmembrane regions during the activation process.

Keywords: β_1-Adrenergic receptor; Mutant receptors; Receptor model; cAMP; Agonist binding; Activation

1. Introduction

In all seven α-helical transmembrane (tm) G-protein-coupled receptors (GPCRs) it appears that the general mechanism of activation involves disruption of intramolecular constraints, leading to tm movement and the formation of new interactions, which stabilize the active state of the receptor [1–14]. Disruption of an interhelical constraint between tms 3 and 7 has been shown to be the primary trigger for the conformational changes in opsins during receptor activation. In bovine rhodopsin, the interhelical constraint is a salt bridge [2,12]. Interhelical constraints between tms 3 and 7 have also been detected in the δ opioid receptor [13] and α_{1b}-adrenergic receptor (α_{1b}-AR) [14].

Our interest lies in β-adrenergic receptors (β-ARs), in particular the β_1-subtype, and we have synthesized several novel and highly specific β_1-AR compounds [15–19]. In the rat β_1-AR, $Trp^{134\ (3.28)}$ and $Tyr^{356\ (7.43)}$ correspond to the two residues involved in the salt bridge formation in bovine rhodopsin [2,12]. $Trp^{134\ (3.28)}$ and $Tyr^{356\ (7.43)}$ are

Abbreviations: β-AR, β-adrenergic receptor; tm, transmembrane; GPCR, G-protein-coupled receptor; cAMP, adenosine 3′:5′-cyclic monophosphate; CHO, Chinese hamster ovary; WT, wild type; M_1, M_1 muscarinic acetylcholine receptor; H_4, histamine H_4 receptor; $5\text{-}HT_{2A}R$, 5-hydroxytryptamine$_{2A}$ receptor; α_{1b}-AR, α_{1b}-adrenergic receptor; G418, geneticin; BSA, bovine serum albumin; ^{125}I-CYP, ^{125}Iodocyanopindolol; GTP, guanosine 5′-triphosphate; K_d, dissociation constant; K_i, inhibition constant; pD_2, functional potency; IA, intrinsic activity; ΔH_f°, heat of formation; (−)-RO363, (−)-1-(3′,4′-dihydroxyphenoxy)-3-(3″,4″dimethoxyphenyl)ethylamino-2-propanol hydrochloride; D150, (±)-3-(4-hydroxyphenoxy)-2-hydroxy-1-(tetrahydropyran-4-carboxamidoethylamino) propane; AOPA, aryloxypropranolamine; AEA, arylethanolamine

* Corresponding author. Tel.: +61 3 94965486; fax: +61 3 94593510.
E-mail address: ajenkins@unimelb.edu.au (W.J. Louis).

0006-2952/$ – see front matter © 2004 Elsevier Inc. All rights reserved.
doi:10.1016/j.bcp.2004.04.021

capable of forming π–π and/or hydrogen bond interactions and this led us to examine whether these two residues contributed to the activation of the β_1-AR. In addition, our earlier β_1-AR molecular modeling studies revealed that both $Trp^{134\ (3.28)}$ and $Tyr^{356\ (7.43)}$ form part of a hydrophobic pocket defined by tms 1, 2, 3 and 7 and that they are ideally located to interact with the amine substituent of large ligands [20,21]. Similar molecular modeling results have been reported for the equivalent residues in the β_2-AR for the non-catechol agonist TA2005 [22].

In the past, tm4 has received little attention in 7tm GPCR structural studies as it appeared as an outlier in the formation of the tm bundle [23,24]. However, movement of tm4 has been associated recently with M_1 muscarinic acetylcholine receptor (M_1) activation [25]. Mutagenesis studies involving the M_1 revealed that several inward facing amino acid side chains on the exofacial side of tm4, including $Trp^{157\ (4.57)}$, are involved in a hydrogen bonding network, which triggers movement and rotation of the tms [25]. In the M_1, $Trp^{157\ (4.57)}$ lies close to $Ile^{161\ (4.61)}$ and $Asp^{99\ (3.26)}$ providing an initial binding site for ligands before they enter the central binding pocket [26]. Mutation of the equivalent residue located at position 4.57 ($Asn^{147\ (4.57)}$) to Tyr in the histamine H_4 receptor (H_4) led to a 50% reduction in the ability of the mutant receptor to respond to histamine; however, there were no changes in the level of receptor expression compared to the wild type (WT) and little effect on binding [27]. $Ser^{207\ (4.57)}$ has been reported to contribute to the formation of a stable agonist–receptor complex in the 5-hydroxytryptamine$_{2A}$ receptor (5-HT_{2A}R), whereas the equivalent residue ($Ala^{187\ (4.57)}$) in the 5-HT_{2B}R has no effect on 5-HT binding affinity or receptor activation [28]. In this study, we investigated whether residue 4.57 in the rat β_1-AR, i.e. $Ser^{190\ (4.57)}$, may play a role in agonist binding and/or receptor activation.

To clarify the role(s) played by $Trp^{134\ (3.28)}$, $Ser^{190\ (4.57)}$ and $Tyr^{356\ (7.43)}$ in the rat β_1-AR we made the following mutations: $Trp^{134\ (3.28)}$ to Ala (W134A), $Ser^{190\ (4.57)}$ to Ala (S190A) and $Tyr^{356\ (7.43)}$ to Phe (Y356F). Although the subject of considerable speculation [22,29], these specific mutations have not been studied previously in the β_1-AR. We measured the effect of the mutations on binding affinity and receptor activation of a range of selective and non-selective β-AR agonists and partial agonists (Fig. 1). A model of the rat β_1-AR, based on the bovine rhodopsin crystal structure [12], was used to visualize initial agonist binding and aid in the interpretation of the experimental results.

2. Materials and methods

2.1. Materials

Drugs and chemicals were obtained from the following manufacturers. Glutamine, HEPES, polyethyleneimine, phosphoenolpyruvate, guanosine 5′-triphosphate (GTP) sodium salt, isobutylmethylxanthine, adenosine 5′-triphosphate (ATP) disodium salt, propanolol, sodium fluoride, (−)-isoprenaline and (−)-norepinephrine from Sigma Chemical Co., forskolin from Boehringer Ingelheim, pindolol and xamoterol were obtained from Tocris Cooksen Ltd. D150 ((±)-3-(4-hydroxyphenoxy)-2-hydroxy-1-(tetrahydropyran-4-carboxamidoethylamino) propane) and (−)-RO363 ((−)-1-(3′,4′-dihydroxyphenoxy)-3-(3″,4″dimethoxyphenyl)ethylamino-2-propanol hydrochloride) were synthesized in our laboratory by Dr. Dimitri Iakovidis

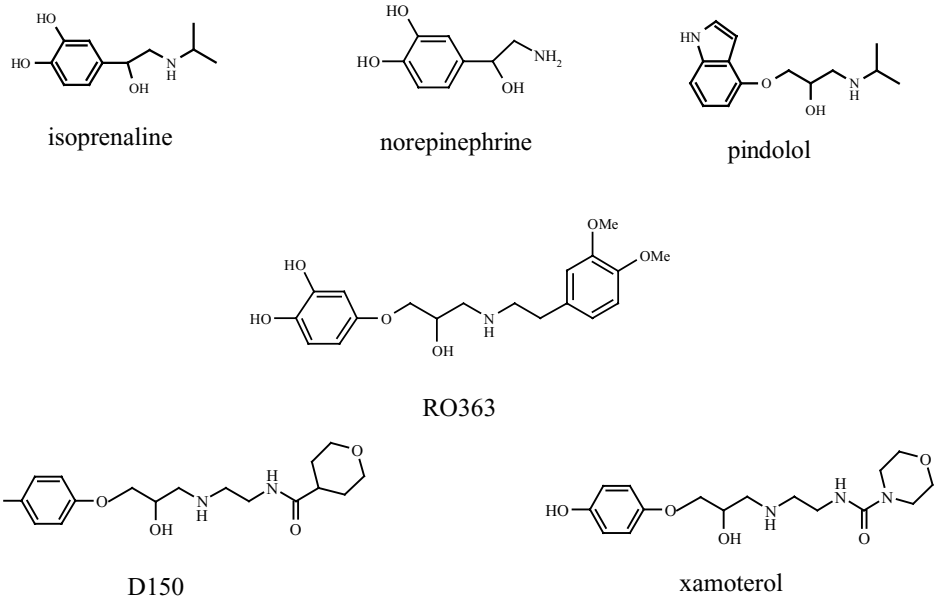

Fig. 1. Chemical structures of the agonists isoprenaline and norepinephrine, and the partial agonists RO363, D150, xamoterol and pindolol.

[15,16]. Unless otherwise indicated, racemates were used. (−)-RO363 and D150 were checked by TLC, HPLC, NMR, elemental analysis and mass spectroscopy and their physical characteristics were consistent with their chemical structure. ^{125}Iodocyanopindolol (^{125}I-CYP) was kindly produced in our department by Mr. David Casley using the chloramine-T/NaI method [30]. Ham's F12, sodium pyruvate, trypsin, penicillin and streptomycin were obtained from Edward Keller; oligonucleotides, geneticin (G418) and the mammalian expression vector pcDNA3.1 from Invitrogen. Adenosine 3′:5′-cyclic monophosphate (cAMP) (^{3}H) assay system kits were obtained from Amersham Pharmacia Biotech; Chinese hamster ovary (CHO) cell line, fetal calf serum and BSA (fraction V) from Commonwealth Serum Laboratories (CSL) and restriction enzymes, *Eco*R1 and *Xba*1 from Promega Corporation. The plasmid construct pGem3Z-β_1 encoding for the rat β_1-AR was kindly provided by Dr. Curtis A. Machida. Quik change site-directed mutagenesis kits were purchased from Stratagene.

2.2. Mutagenesis of rat β_1-AR cDNA

For receptor expression, the entire coding region derived from pGem3Z-β_1 (base pairs −82 to +1573) was inserted into the *Eco*R1 and *Xba*1 sites of the mammalian vector pcDNA3.1, which provides G418 selection. The mutations of Trp$^{134\ (3.28)}$, Ser$^{190\ (4.57)}$ and Tyr$^{356\ (7.43)}$ to W134A, S190A and Y356F, respectively were generated using the Quik change method according to the manufacturer's instructions. The identities of the mutations were confirmed by automated sequencing on an ABI sequencer.

2.3. Cell culture and transfection

Transfected CHO cells were grown at 37 °C in a 10% CO_2 incubator in Ham's F12 media, supplemented with 10% fetal calf serum, 2 mM glutamine, 1 mM sodium pyruvate, 100 units/ml penicillin, 100 μg/ml streptomycin and 800 μg/ml G418. WT and mutant plasmids were stably transfected into CHO cells by electroporation. Colonies originating from single cells were subcloned and evaluated for receptor expression using ^{125}I-CYP binding.

2.4. Preparation of crude cell membranes

Membranes were prepared from preconfluent, stably transfected CHO cells washed twice with ice-cold phosphate buffer solution, harvested with 25 mM Tris–HCl, pH 7.5, 1 mM EDTA buffer, homogenized with 20 strokes of a Dounce pestle, and then centrifuged at 10,000 × *g* for 15 min. The final membrane pellets were resuspended in Hank's balanced salt solution and stored at −80 °C [31]. Cells were thawed as required and resuspended in Hank's balanced salt solution supplemented with 20 mM HEPES and 0.1% (mass/volume) BSA at 100–200 μg protein per millilitre for all studies. Protein content was determined by the Bradford method [32] using BSA as the standard.

2.5. Radioligand binding studies

In saturation binding studies, 0.1 ml of membranes were incubated in duplicate with increasing concentrations of ^{125}I-CYP (2 pM–1 nM). Competition binding experiments were conducted as previously described [31]. Cell membranes were incubated with 100 pM ^{125}I-CYP and various concentrations of competing ligand in a final volume of 0.2 ml. All determinations were done in triplicate. Membranes were incubated for 1 h at 37 °C in the dark and the assay terminated by rapid filtration over glass fibre filters presoaked with (0.1%) polyethyleneimine. Non-specific binding was determined in the presence of 10 μM propranolol.

2.6. cAMP accumulation assays

cAMP accumulation was measured in whole cells. Cells equivalent to 5 μg of protein were incubated for 15 min at 37 °C in a final volume of 1 ml of HEPES double strength buffer pH 7.6 containing 0.33 mM phosphoenolpyruvate, 5 mM GTP, 0.25 mM $MgCl_2$, 0.5 mM KCl, 0.05 mM isobutylmethylxanthine, 0.0125 mM ATP and various concentrations of the agonist (−)-isoprenaline. For each cell line, forskolin (30 μM) and NaF (10 mM)-induced activation of basal adenylyl cyclase production was measured. All determinations were done in duplicate. In addition, the effect of adding 10 μM propranolol or 10 μM betaxolol to unstimulated CHO cells stably transfected with WT or mutant rat β_1-ARs was examined to determine the level of constitutive activation.

2.7. Data analysis

Data are expressed as the mean ± standard error of the mean (S.E.M.) of three to five independent experiments. Dissociation constant (K_d) (saturation studies), inhibition constant (K_i) (drug inhibition) and receptor binding density (B_{max}) values were determined using the computerized iterative curve fitting program EBDA (version 4.0), which incorporates LIGAND version 4.0 [33,34]. Pseudo Hill coefficients (n_H) were obtained from analysis of binding data using the sigmoidal fit function of the EBDA program. Functional potency (pD_2) and intrinsic activity (IA) were determined using Graphpad Prism software (version 3.0).

2.8. Statistical analysis

The K_d, pK_i, B_{max}, IA, pD_2 and basal adenylyl cyclase activation values in the mutant versus WT receptors were compared by one-way ANOVA followed by pairwise Tukey's test using the Analysis-IT software for Microsoft Excel. Critical values of $P < 0.05$ defined statistical

significance. Correlations were performed on mean mutant versus WT receptor values using the linear regression function of Microsoft Excel. The response variable "percentage maximum of WT isoprenaline-basal" (Fig. 4C and D) was also analyzed. These percentages ranged from 0% to 100%; accordingly, a transformation of the response variable was used to justify the assumptions of analysis of variance. The usual transformation for such data is the logit transformation; if the percentage is y then, $\text{logit}(y) = \log(y/(100 - y))$. However, the presence in the data of observations at the extreme values of 0% and 100% means that a slight modification is necessary; the actual transformation used was $f(y) = \log((y + 0.5)/(100 - y + 0.5))$ [35]. This transformed variable was analyzed using dose and group as explanatory variables in a two-way ANOVA.

2.9. Homology modeling of the WT rat β_1-AR

A three-dimensional homology model of the 7tm regions of the rat β_1-AR was constructed using the crystal structure of inactive bovine rhodopsin (PDB file 1F88; [12]) as a template; hence, the rat β_1-AR model was also presumed to be in an inactive conformation. Loop regions were not included. The 7tm sequences of the rat and human β_1-AR, human β_2-AR and bovine rhodopsin were aligned as in Fig. 2 (consistent with Palczewski et al. [12]). Pairwise amino acid similarity of the tm regions between the rat and human β_1-AR was 90% (94% allowing for conservative substitution), 66% between the rat β_1-AR and human β_2-AR (79% allowing conservative substitutions) and 69% between the human β_1-AR and β_2-AR (82% allowing conservative substitutions). By comparison, there was 23% sequence identity between bovine rhodopsin and the rat β_1-AR (46% allowing conservative substitution), 24% between bovine rhodopsin and the human β_1-AR (47% allowing conservative substitution) and 24% between bovine rhodopsin and the human β_2-AR (49% allowing conservative substitution). The amino acid sequence of the bovine rhodopsin crystal structure was mutated to that of the rat β_1-AR using the mutate functionality in the Biopolymer module of the modeling program SYBYL (version 6.8, Tripos Assoc Inc.). In tm1 of bovine rhodopsin, $\text{Ala}^{(1.36)}$ was excised from the helix in order to maintain the alignment of the conserved $\text{Trp}^{(1.30)}$, $\text{Met}^{(1.34)}$, $\text{Leu}^{(1.41)}$, $\text{Asn}^{(1.50)}$ and $\text{Leu}^{(1.52)}$ residues (Fig. 2). The resulting rat β_1-AR tm1 was annealed in the region of the excision site and compared to the bovine rhodopsin tm1 to confirm that conserved residues were still in alignment. Excision or inclusion of $\text{Ala}^{(1.36)}$ in the construction of the β_1-AR model does not affect our modeling results as the extracellular end of tm1 does not appear to be involved in the ligand-binding site. The crude rat β_1-AR model was then subjected to molecular mechanics minimization using the following parameters; Kollman all atom force field and atomic charges, conjugate gradient minimization, distance dielectric function and a dielectric constant of 5.0, non-bonded cut off 8 Å and 2000 maximum iterations (the same molecular mechanics parameters were used when annealing the section of tm1 described above). After minimization, the rat β_1-AR model was superimposed onto the bovine rhodopsin crystal structure via the backbone atoms and the resulting RMS was 0.8 Å.

For hydrogen bond interactions, donor–acceptor distances of 3.0–4.0 Å were considered to be feasible. Distances of 4.0–7.0 Å between ring centroids were deemed acceptable for aromatic–aromatic interactions.

In most instances, the amino acid residues have been dually numbered. In superscript, they are numbered according to their position in the receptor sequence and in brackets they have been given a number corresponding to their relative position in the helix [36]. In this universal numbering system, every amino acid number begins with the tm number, followed by a number which defines their position relative to the most conserved residue in that tm. The reference residue is assigned the number 50.

2.10. Docking agonists into the WT rat β_1-AR ligand-binding site

Detailed experimental data outlining conformational changes for the GPCR and agonist during receptor activation are not yet available [4,5,10,11,22]. The initial interactions between the agonist and the inactive receptor state were investigated and modeled in this study. Active agonist isomers, i.e. *R*-(−)-isoprenaline, *R*-(−)-norepinephrine, *S*-D150, *S*-(−)-RO363, *S*-xamoterol and *S*-pindolol were constructed within the sketch functionality of SYBYL in a fully extended conformation. Agonists were structurally optimized first using the Tripos molecular mechanics force field and Gasteiger–Huckel atomic charges (all other parameters were left at default values), and then using the AM1 Hamiltonian within the MOPAC (version 6.00) program as supplied with SYBYL. Parameters used for the semi-empirical molecular orbital calculations were as follows: AM1 Hamiltonian, precise convergence, no molecular mechanics correction for amide linkages and full geometry optimization.

Individual agonists were then manually docked into the rat β_1-AR ligand-binding site, allowing agonist torsion angles to vary in order to maximize putative initial agonist–receptor interactions (these interactions are described in Section 2.11). Once the agonist was docked, the entire agonist–receptor complex was subjected to molecular mechanics minimization following the same protocol as for the model construction, with the exceptions that the Tripos force field, Gasteiger–Huckel atomic charges and 1000 maximum iterations were used. For each agonist several different binding modes were examined.

Agonist molecules were extracted out of the minimized agonist–receptor complex and the heat of formation (ΔH_f°) calculated for the bound agonist conformation using the

tm1	β_1-AR rat	57	**W**TAG**M**G-LLLA**L**IVLLIVVG**N**V**L**VIVAIAK	85
	β_1-AR human	57	**W**TAG**M**G-LLMA**L**IVLLIVAG**N**V**L**VIVAIAK	85
	β_2-AR human	32	**W**VVG**M**G-IVMS**L**IVLAIVFG**N**V**L**VITAIAK	60
	Bovine rhodopsin	35	**W**QFS**M**LAAYMF**L**LIMLGFPI**N**F**L**TLYVTVQ	64
tm2	β_1-AR rat	92	LT**N**LFIMS**L**A**S**A**D**LVM**G**LLVVPFGATIVVW	121
	β_1-AR human	92	LT**N**LFIMS**L**A**S**A**D**LVM**G**LLVVPFGATIVVW	121
	β_2-AR human	67	VT**N**YFITS**L**AC**A**D**L**VM**G**LAVVPFGAAHILM	96
	Bovine rhodopsin	71	PL**N**YILLN**L**AV**A**D**L**FM**V**FGGFTTTLYTSLH	100
			*	
tm3	β_1-AR rat	128	SFF**C**ELWTSVDV**L**CVTASIET**L**C**V**I**A**LD**R**YLAI	160
	β_1-AR human	128	SFF**C**ELWTSVDV**L**CVTASIET**L**C**V**I**A**LD**R**YLAI	160
	β_2-AR human	103	NFW**C**EFWTSIDV**L**CVTASIET**L**C**V**I**A**VD**R**YFAI	135
	Bovine rhodopsin	107	PTG**C**NLEGFFAT**L**GGEIALWS**L**V**V**L**A**IE**R**YVVV	139
			*	
tm4	β_1-AR rat	173	AR**A**RALVCTV**W**AISALVSFL**P**IL	195
	β_1-AR human	173	AR**A**RGLVCTV**W**AISALVSFL**P**IL	195
	β_2-AR human	148	NK**A**RVIILMV**W**IVSGLTSFL**P**IQ	170
	Bovine rhodopsin	151	NH**A**IMGVAFT**W**VMALACAAP**P**LV	173
tm5	β_1-AR rat	221	**N**RAYA**I**ASSV**V**S**F**YV**P**L**C**IMA**F**V**Y**LR	246
	β_1-AR human	221	**N**RAYA**I**ASSV**V**S**F**YV**P**L**C**IMA**F**V**Y**LR	246
	β_2-AR human	196	**N**QAYA**I**ASSI**V**S**F**YV**P**L**V**IMV**F**V**Y**SR	221
	Bovine rhodopsin	200	**N**ESFV**I**YMFV**V**H**F**II**P**L**I**VIF**F**C**Y**GQ	225
tm6	β_1-AR rat	308	**E**QKALKTLG**I**IMGV**F**TL**C**W**L**P**F**FLANVVKAF	338
	β_1-AR human	319	**E**QKALKTLG**I**IMGV**F**TL**C**W**L**P**F**FLANVVKAF	349
	β_2-AR human	268	**E**HKALKTLG**I**IMGT**F**TL**C**W**L**P**F**FIVNIVHVI	298
	Bovine rhodopsin	247	**E**KEVTRMVI**I**MVIA**F**LI**C**W**L**P**Y**AGVAFYIFT	277
			*	
tm7	β_1-AR rat	346	RLFVFFNWLGYANSAF**N**P**I**I**Y**	366
	β_1-AR human	357	RLFVFFNWLGYANSAF**N**P**I**I**Y**	377
	β_2-AR human	306	EVYILLNWIGYVNSGF**N**P**L**I**Y**	326
	Bovine rhodopsin	286	IFMTIPAFFAKTSAVY**N**P**V**I**Y**	306

Fig. 2. Alignment of the 7tm regions for the rat and human β_1-AR, human β_2-AR and bovine rhodopsin. The amino acid sequence numbers for the start and finish of the tms for each individual receptor are included. Residues conserved in all four receptors are highlighted in bold. The location of the three rat β_1-AR residues which have been mutated in this study are indicated by the presence of an asterix (directly above). The universal numbering system reference residue for each tm region has been underlined.

AM1 Hamiltonian within MOPAC. Parameters used for the semi-empirical molecular orbital calculations were as for those described above for the fully extended agonist conformations, except torsion angles were not optimized in bound conformations. For each agonist, the ΔH_f° for the various bound conformations was compared to the ΔH_f° of the fully extended conformation to ensure that the bound conformation was energetically feasible (i.e. within 10 kcal/mol of the fully extended conformation. Bound conformations with a ΔH_f° more than 10 kcal/mol higher were considered to be unrealistic and discarded).

2.11. Validation of the WT rat β_1-AR model

The minimized model of the 7tm regions of the rat β_1-AR in a putative inactive conformation is shown in Fig. 3A, with *R*-(−)-isoprenaline (red) docked into the ligand-binding site. α-Helices are depicted in a grey ribbon representation, with important side chain residues coloured blue and the three mutated residues coloured green. The agonist binding site is located approximately one-third of the way from the extracellular surface (Fig. 3B). Residues previously shown to be important for agonist binding were located in positions in the rat β_1-AR model consistent with

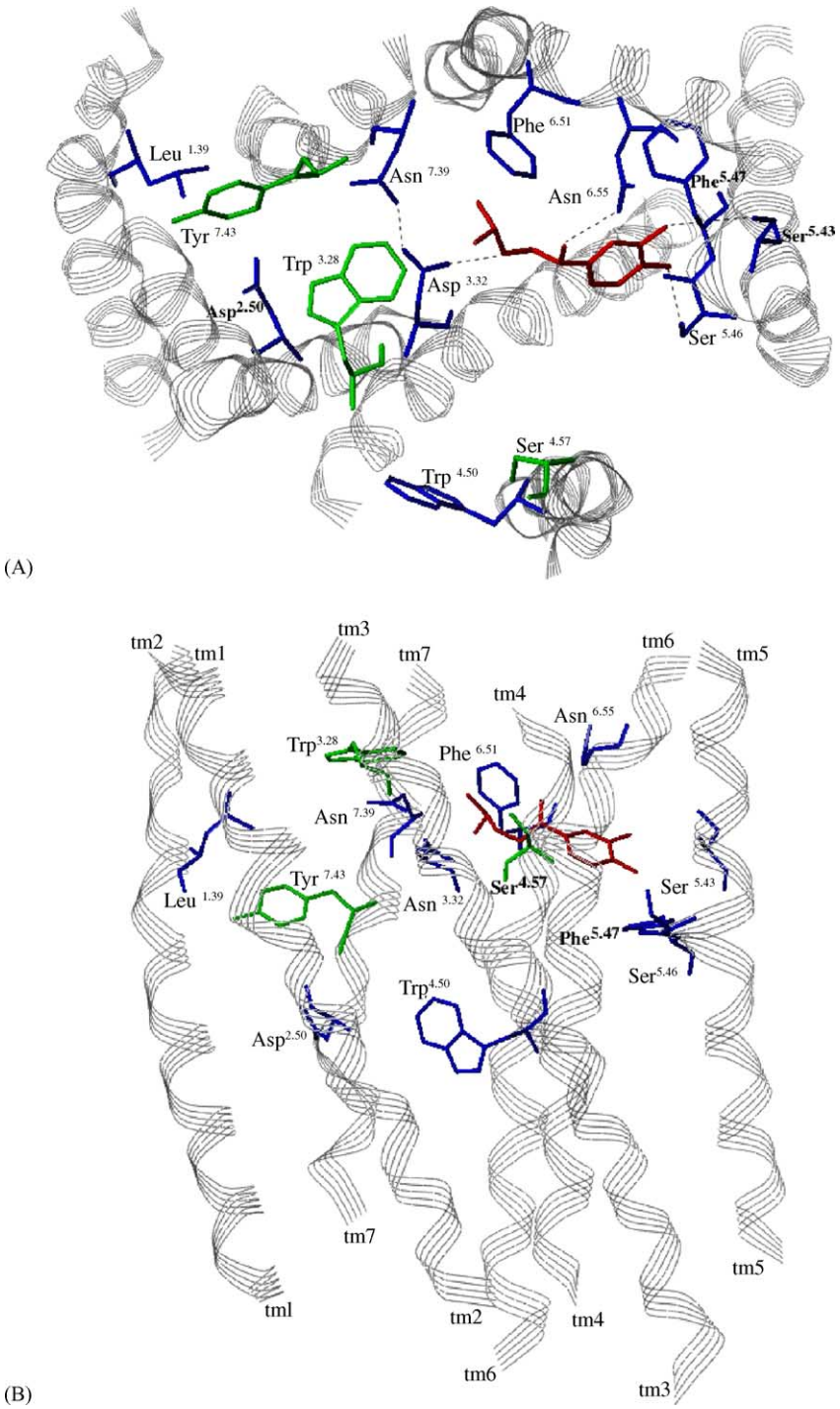

Fig. 3. Model of the 7tm regions of the WT rat β_1-AR with *R*-(−)-isoprenaline (red) docked into the ligand-binding site. The tm regions are shown as grey ribbons. The three residues mutated in this study are shown in green. Residues shown in blue are some of the residues discussed in the text. Putative interactions discussed in the text are displayed as dashed lines. Donor–acceptor distances of 3.0–4.0 Å were considered to be feasible for hydrogen bonding. Hydrogen atoms are not displayed. (A) An extracellular view looking down through the ligand-binding site. (B) 90° rotation about the *x*-axis of A, i.e. side view of (A) through the membrane, the end of each tm region has been labeled.

their proposed roles: $Asp^{138\ (3.32)}$ interacting with the agonist amino group [4,10,23,37]; $Ser^{229\ (5.43)}$, $Ser^{228\ (5.42)}$ and $Ser^{232\ (5.46)}$ hydrogen bonding with the hydroxyl groups of the agonist's catechol moiety [4,10,23,37–40]; $Asn^{333\ (6.55)}$ interacting with the agonist β-hydroxyl group [4,41]; $Phe^{233\ (5.47)}$, $Phe^{329\ (6.51)}$ and $Phe^{330\ (6.52)}$ forming an aromatic pocket into which the agonist's catechol ring can be accommodated [23,42,43].

Our model is consistent with several recent β-AR molecular modeling studies [22,36,44,45] and also with proposed receptor activation mechanisms for GPCRs [1–11,46]. $Arg^{156\ (3.50)}$ is part of the E/DRY

Table 1
Effects of single point mutations of the rat β_1-AR on ligand binding for a range of β-AR agonists and partial agonists

	^{125}I-CYP		Ligands (pK_i)					
	K_d (pM)	B_{max} (fmol/mg)	(−)-Isoprenaline	(−)-Norepinephrine	D150	(−)-RO363	Xamoterol	Pindolol
WT	61 ± 2	417 ± 132	6.5 ± 0.03	5.1 ± 0.02	5.7 ± 0.02	7.3 ± 0.1	7.0 ± 0.1	8.8 ± 0.1
Y356F	85 ± 14	256 ± 30	5.2 ± 0.1**	5.0 ± 0.1	4.6 ± 0.1**	6.9 ± 0.1*	4.9 ± 0.1**	7.8 ± 0.1*
W134A	63 ± 5	570 ± 70	5.9 ± 0.1*	4.6 ± 0.1*	5.8 ± 0.1	7.5 ± 0.02	6.1 ± 0.1*	8.2 ± 0.1*
S190A	64 ± 7	379 ± 5.3	5.4 ± 0.1**	4.3 ± 0.1**	5.6 ± 0.1	6.4 ± 0.1**	6.1 ± 0.1*	7.8 ± 0.04*

The binding affinity (pK_i) was determined by the inhibition of 100 pM ^{125}I-CYP. Data were analyzed using the non-linear regression program LIGAND [33,34]. Pseudo Hill coefficients (n_H) gave slope values that were not significantly different from unity. Each value represents the mean ± S.E.M. for three to five separate experiments.

* $P < 0.05$.

** $P < 0.01$ compared with the WT rat β_1-AR.

motif located on the cystosolic end of tm3 and is known to be involved in receptor activation. Arg$^{156\ (3.50)}$ is able to interact with both Asp$^{155\ (3.49)}$ and also Glu$^{308\ (6.30)}$, as proposed previously for the equivalent residues in the α_{1b}-AR [2,8,46–48]. The conserved Pro$^{328\ (6.50)}$ in tm6 induces a kink in our model approximately half way along the helix consistent with the Greasley et al. [46] proposal for the α_{1b}-AR. The kink results in the cytosolic end of tm6 being closer to tm3 than the extracellular end. Mutation of this Pro$^{(6.50)}$ to Ala results in constitutive activation of both the α_{1b}-AR and yeast α-factor receptor [11], suggesting the kink induced by Pro$^{(6.50)}$ is important for receptor activation. It has been suggested that the tm6 kink and the rigidity produced by Pro$^{(6.50)}$ acts as a pivot for amplification of the receptor conformational changes upon agonist binding and also for productive propagation of the agonist signal to the G-protein interacting with the tm6–cytoplasmic receptor interface [2,8,11,48]. Our model allows Pro$^{328\ (6.50)}$ to play a similar role in the rat β_1-AR.

The location of Tyr$^{366\ (7.53)}$ in the rat β_1-AR model is consistent with its proposed role in receptor sequestration [49], i.e. it is located at the cytosolic end of tm7 and points towards the lipid bilayer. In our model, the side chain of Trp$^{183\ (4.50)}$ (a conserved residue in GPCRs, Figs. 2 and 3A) passes behind tm3 pointing towards tm2 and its orientation is consistent with the suggestion that the equivalent residue in bovine rhodopsin (Trp$^{161\ (4.50)}$) helps stabilize the orientation of tm3 not only with respect to tm4 but also tm2 [2,12].

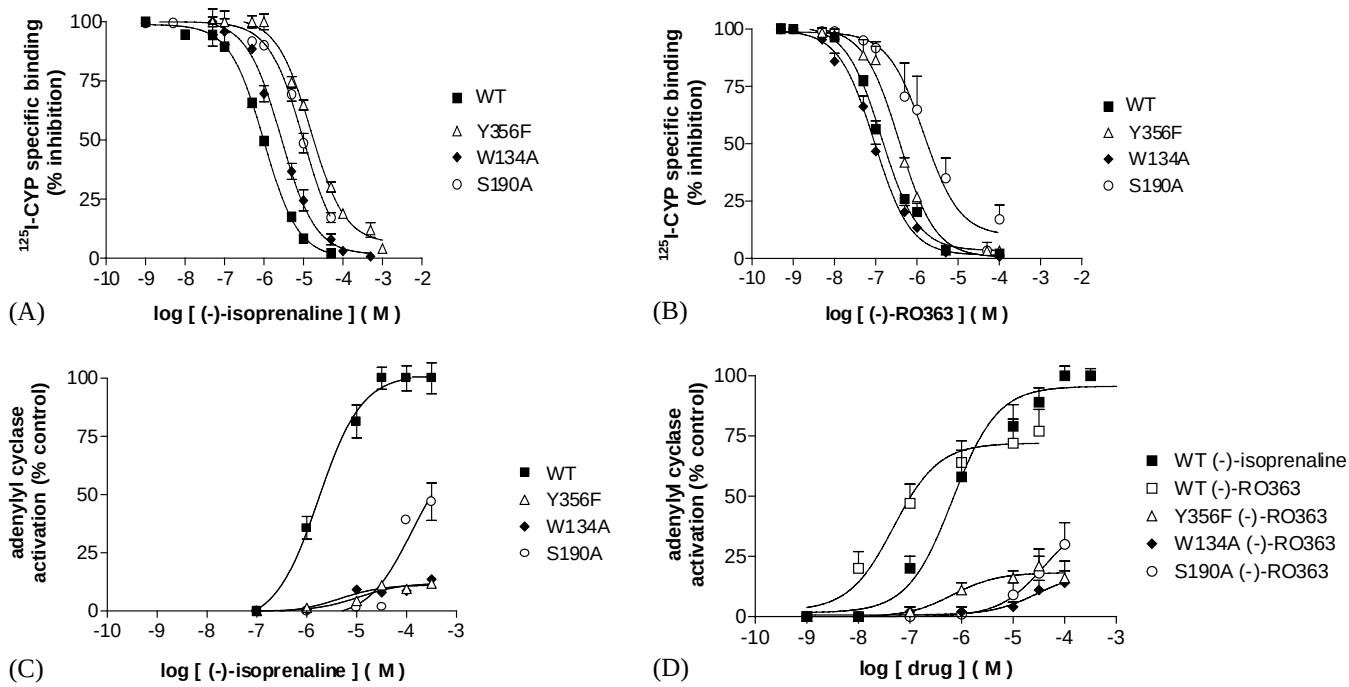

Fig. 4. Inhibition of specific ^{125}I-CYP binding by (A) (−)-isoprenaline, (B) (−)-RO363 in membranes expressing WT or mutant rat β_1-ARs. The binding parameters are shown in Table 1. Data points are mean ± S.E.M. of $n = 3$–5 experiments of triplicate determinations. The bottom panels display adenylyl cyclase activation induced by (C) (−)-isoprenaline and (D) (−)-RO363 in WT and mutant β_1-ARs. Data points are presented as a percentage of the maximal response to (−)-isoprenaline in WT β_1-ARs and are mean ± S.E.M. of $n = 3$–5 experiments of duplicate determinations (see Tables 1 and 2 for P-values).

3. Results

3.1. Radioligand binding assays

Saturation studies of the WT rat β_1-AR and all three mutant receptors revealed that the mutations did not significantly ($P > 0.05$) affect the affinity (K_d) for ^{125}I-CYP or receptor density (B_{max}) compared to WT (Table 1) and that ^{125}I-CYP bound to a single population of binding sites in each case ($n_H = 0.90 - 1$).

Competition binding experiments with a range of agonists also defined monophasic inhibition curves (Fig. 4A and B, $n_H = 0.89 - 1$). The exception was the Y356F mutant, where preferred binding site parameters could not be determined statistically for xamoterol as the inhibition curves were incomplete at $10^{-4.5}$ M due to its poor affinity for this mutant. To confirm the monophasic curves for (−)-isoprenaline, competition binding studies were also conducted using a wider range (1 nM–1 mM) of (−)-isoprenaline concentrations (18 data points, data not shown) in both the absence and presence of guanine nucleotides (GTP). In every case (−)-isoprenaline inhibited ^{125}I-CYP binding in a monophasic fashion ($n_H = 0.88 - 1$).

The impact of the amino acid substitutions on ligand binding was further evaluated by determining the affinity (pK_i) of the mutant receptors for a range of β-AR agonists and partial agonists (Table 1, Fig. 1). Except for xamoterol in the Y356F mutant, the three mutations had relatively small and statistically variable effects on pK_i and the change in affinity, compared to WT, for the agonists ranged from a 20-fold decrease to a 2-fold increase (Table 1).

The reduction in binding affinity displayed by the β_1-selective partial agonist xamoterol for the Y356F mutant was quite dramatic and highly significant; the pK_i was 7.0 ± 0.1 in the WT and this was reduced to 4.9 ± 0.1 in the mutant (126-fold, $P < 0.01$). The reduction in xamoterol binding for the Y356F mutant was 15-fold greater than the pK_i reduction observed for the W134A and S190A mutants. In comparison, the pK_i of D150 (a xamoterol analogue and also a β_1-selective partial agonist) fell from 5.7 ± 0.02 in the WT receptor to 4.6 ± 0.1 (12-fold, $P < 0.01$) for the Y356F mutant receptor.

3.2. cAMP assays

In the untransfected CHO cells, (−)-isoprenaline and (−)-RO363 were unable to stimulate adenylyl cyclase consistent with the absence of endogenous β-ARs. There were no significant differences between the mutant and WT receptors in forskolin (30 μM) or NaF (10 mM)-induced adenylyl cyclase activation (data not shown), indicating that the β_1-AR independent mechanism of adenylyl cyclase activation was intact. Basal adenylyl cyclase activity was not significantly different in WT and mutant receptors (Table 2). The inability of propranolol or betaxolol to inhibit basal cAMP accumulation in CHO cells transfected with either WT or mutant rat β_1-ARs suggests that there is little or no constitutive activation in our system (data not shown).

In preliminary studies, we found that the partial agonists xamoterol and D150 produced no significant agonist effect in this assay, presumably because their IA in this system was too low. We decided to focus the adenylyl cyclase stimulation studies on the two agonists (−)-isoprenaline and (−)-RO363 (Table 2, Fig. 4C and D), as they had easily measurable responses in this assay. The ability of (−)-isoprenaline and (−)-RO363 to stimulate adenylyl cyclase, measured as IA and pD_2, was significantly lower for the three mutants than for the WT receptor (for P-values refer to Table 2); with the exception of the (−)-isoprenaline pD_2 for the W134A mutant. The functional potency of the compounds for the mutant receptors was difficult to estimate due to the weak agonist effects. In spite of this, there was a significant correlation between change in IA and change in pD_2 compared to WT values for (−)-isoprenaline and (−)-RO363 ($r^2 = 0.7$, $P = 0.04$). The effect on the IA of (−)-isoprenaline was significantly different ($P < 0.01$) to WT for all three mutants. The S190A mutant was the least affected, where (−)-isoprenaline induced 47% of the WT receptor maximal response and this was significantly different ($P < 0.01$) from both the Y356F (12%) and W134A (14%) mutant receptors, respectively (Table 2).

Table 2
The functional potency (pD_2) and intrinsic activity (IA) of (−)-isoprenaline and (−)-RO363 at WT and mutant rat β_1-ARs

	Basal adenylyl cyclase activity (%WT)	Ligands			
		(−)-Isoprenaline		(−)-RO363	
		pD_2 (M)	IA (%WT)	pD_2 (M)	IA (%WT)
WT	100	5.9 ± 0.1	100	7.5 ± 0.3	79 ± 11
Y356F	86 ± 20	4.7 ± 0.3**	12 ± 5.8**	6.0 ± 0.1*	21 ± 2**
W134A	86 ± 21	5.5 ± 0.2	14 ± 1.5**	4.4 ± 1.0**	18 ± 3**
S190A	79 ± 30	3.9 ± 0.1**	47 ± 8.0**	4.2 ± 1.0**	33 ± 10*

pD_2, log concentration of agonist inducing half maximal adenylyl cyclase activation; IA, percentage maximum effect of agonist on adenylyl cyclase activity as compared to maximum effect of (−)-isoprenaline. Values are mean ± S.E.M. of three to five experiments. Basal adenylyl cyclase activity is expressed as a %WT, which is defined as 100%. There were no significant differences between the mutants and WT in basal adenylyl cyclase activity, $P > 0.05$.

* $P < 0.05$.

** $P < 0.01$ compared with the WT rat β_1-AR.

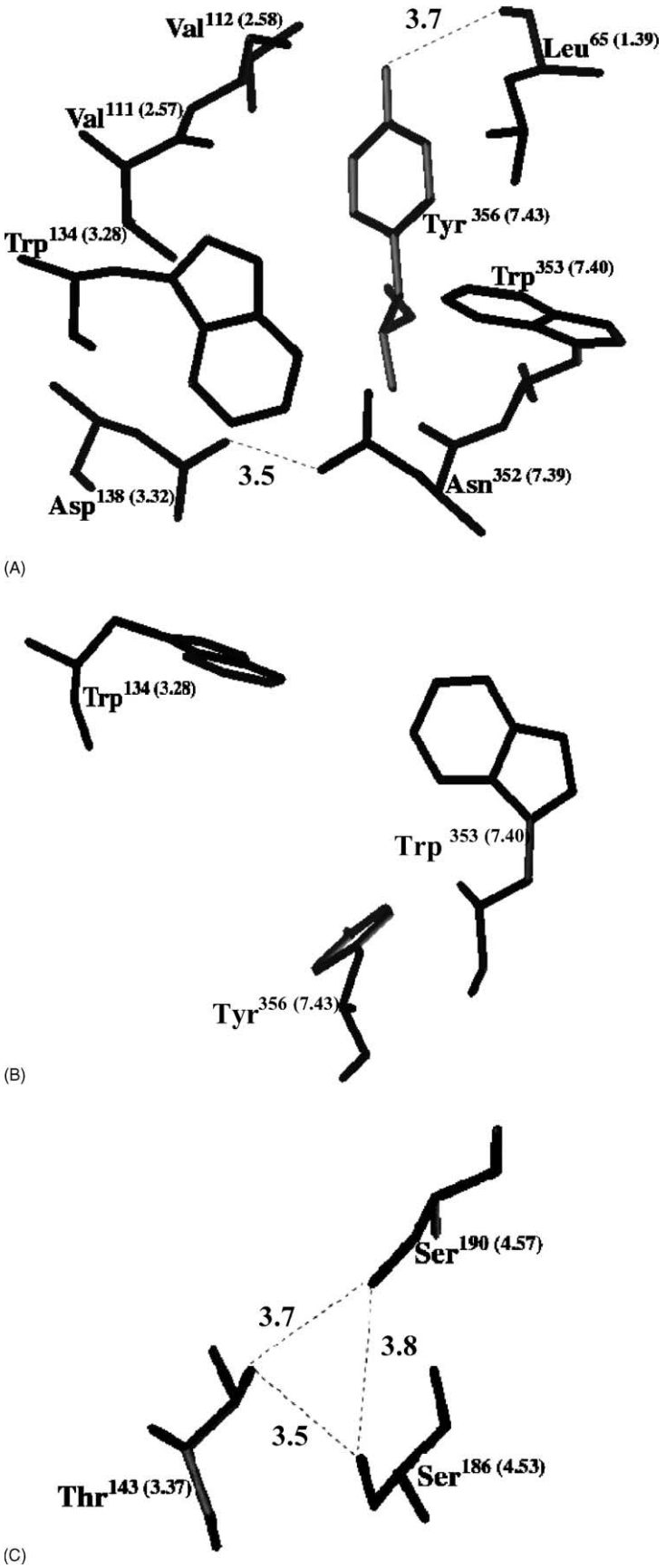

Fig. 5. Environment of the three residues mutated in this study in the ligand-free, WT rat β_1-AR model. (A) Aromatic cluster at the extracellular ends of tms 3 and 7. Trp$^{134\ (3.28)}$ interacts with both Trp$^{353\ (7.40)}$ (edge-to-face interaction) and Asn$^{352\ (7.39)}$ (cation–π interaction). Asn $^{352\ (7.39)}$ is also able to hydrogen bond with Asp$^{138\ (3.32)}$. Tyr$^{356\ (7.43)}$ interacts with Trp$^{353\ (7.40)}$ (edge-to-face interaction) and the Tyr$^{356\ (7.43)}$ hydroxyl group hydrogen bonds to the carbonyl

There was no significant difference between the Y356F and W134A mutants. When compared to WT, the fall in IA for (−)-RO363 was significant, $P < 0.05$ for the S190A mutant and $P < 0.01$ for the other two mutants (Table 2); however, there was no significant difference in the IA between the three mutants.

In addition, there was no correlation between changes in IA and pK_i for either (−)-isoprenaline ($r^2 = 0.11$, $P = 0.37$) or (−)-RO363 ($r^2 = 0.02$, $P = 0.70$) or changes in pD_2 and pK_i for either agonist ($r^2 = 0.48$, $P = 0.51$ and $r^2 = 0.11$, $P = 0.78$, respectively).

3.3. Location of the mutated residues in the WT rat β_1-AR model

In the rat β_1-AR model, $Trp^{134\ (3.28)}$ is located at the extracellular end of tm3 and forms part of a hydrophobic pocket in the ligand-binding site defined by $Leu^{65\ (1.39)}$, $Met^{107\ (2.53)}$, $Val^{111\ (2.57)}$, $Val^{112\ (2.58)}$, $Asn^{352\ (7.39)}$, $Trp^{353\ (7.40)}$ and $Tyr^{356\ (7.43)}$ (Fig. 3A and B). $Trp^{134\ (3.28)}$ forms an edge-to-face aromatic interaction with $Trp^{353\ (7.40)}$ (distance between the six-membered ring centroids is 6.1 Å, Fig. 5A and B) and a cation–π interaction with $Asn^{352\ (7.39)}$ (distance between the $Trp^{134\ (3.28)}$ six-membered ring centroid and the functional group of $Asn^{352\ (7.39)}$ is 4.3 Å). Replacing $Trp^{134\ (3.28)}$ with Ala results in the removal of these two interactions between the extracellular ends of tms 3 and 7.

$Tyr^{356\ (7.43)}$ is located approximately half way along tm7 and usually points towards tms 1 and 2 (Fig. 3A and B). When pointing in this direction the hydroxyl group of $Tyr^{356\ (7.43)}$ can hydrogen bond to the carbonyl group of $Leu^{65\ (1.39)}$ in the tm1 helix backbone (Fig. 5A). In addition to the edge–to–face interaction with $Trp^{134\ (3.28)}$, $Trp^{353\ (7.40)}$ also interacts with $Tyr^{356\ (7.43)}$ in a similar manner (distance between the six-membered ring centroids is 6.8 Å, Fig. 5A and B). Mutation of $Tyr^{356\ (7.43)}$ to Phe maintains the aromatic interaction with $Trp^{353\ (7.40)}$, but removes the hydrogen bond to the tm1 helix backbone.

$Ser^{190\ (4.57)}$ is located near the extracellular end of tm4, pointing towards tm3 (Fig. 3A). Closer inspection of the $Ser^{190\ (4.57)}$ environment in the model shows that it is part of a hydrogen bond network, which involves $Thr^{143\ (3.37)}$ and $Ser^{186\ (4.53)}$ (Fig. 5C). Mutation of $Ser^{190\ (4.57)}$ to Ala disrupts this hydrogen bonding network between tms 3 and 4.

3.4. Putative initial agonist interactions in the WT rat β_1-AR model

We assumed that interactions with $Asp^{138\ (3.32)}$, $Asn^{333\ (6.55)}$, $Ser^{229\ (5.43)}$ and/or $Ser^{232\ (5.46)}$ were essential for initial agonist binding when manually docking the agonist molecules into the rat β_1-AR ligand-binding site. Unlike the agonists (−)-isoprenaline, (−)-norepinephrine and (−)-RO363, which all contain a catechol moiety; xamoterol and D150 have only a *para*-hydroxyl group on the phenyl ring (Fig. 1). The indole ring nitrogen of pindolol has been assumed to emulate the *meta*-hydroxyl group of catechol agonists. For each agonist, different interactions were examined for the catechol hydroxyls/*para*-hydroxyl group/indole ring nitrogen with $Ser^{228\ (5.42)}$, $Ser^{229\ (5.43)}$ and $Ser^{232\ (5.46)}$; for example, docking *S*-xamoterol so that the *para*-hydroxyl was able to hydrogen bond to $Ser^{232\ (5.46)}$, and then docking *S*-xamoterol so that the *para*-hydroxyl was hydrogen bonding to $Ser^{229\ (5.43)}$. *R*-(−)-Norepinephrine and *S*-pindolol were docked into the rat β_1-AR ligand-binding site in a similar fashion to that shown in Fig. 3A for *R*-(−)-isoprenaline.

When docking *S*-xamoterol in an extended conformation into the rat β_1-AR ligand-binding site it was found that while maintaining the interaction between $Ser^{232\ (5.46)}$ and the xamoterol *para*-hydroxyl group, the morpholino ring of the amine substituent was able to bind deeply into the hydrophobic binding pocket defined by $Leu^{65\ (1.39)}$, $Met^{107\ (2.53)}$, $Val^{111\ (2.57)}$, $Val^{112\ (2.58)}$, $Trp^{134\ (3.28)}$, $Asn^{352\ (7.39)}$ and $Trp^{353\ (7.40)}$ and hydrogen bond with the $Tyr^{356\ (7.43)}$ hydroxyl group (Fig. 6A). In contrast, *S*-(−)-RO363 is slightly shorter in length than *S*-xamoterol (Fig. 1) and the tetrahydropyran ring of *S*-D150 adopts a different conformation to the xamoterol morpholino ring (Fig. 7). When interactions with $Asp^{138\ (3.32)}$, $Asn^{333\ (6.55)}$, $Ser^{229\ (5.43)}$ and/or $Ser^{232\ (5.46)}$ are maintained, *S*-D150 and *S*-(−)-RO363 are only able to bind to the entrance of the hydrophobic pocket (defined above) and are unable to interact directly with $Tyr^{356\ (7.43)}$ (Fig. 6B). An interaction of xamoterol with the $Tyr^{356\ (7.43)}$ hydroxyl group is consistent with the significant loss in binding affinity (126-fold) of the Y356F mutant (Table 1), compared to WT rat β_1-AR.

S-(−)-RO363, *S*-D150, *S*-xamoterol and *S*-pindolol all belong to the structural class of aryloxypropranolamines (AOPAs) and when docked into the WT rat β_1-AR ligand-binding site they are also able to interact with $Asn^{352\ (7.39)}$. $Asn^{352\ (7.39)}$ is ideally placed to interact with the AOPA amino group, so that the amino group is effectively held into place by an interaction with $Asn^{352\ (7.39)}$ from above and an interaction with $Asp^{138\ (3.32)}$ from below (Fig. 6A and B). The endogenous agonist *R*-(−)-norepinephrine, and many of the shorter agonists like *R*-(−)-isoprenaline, belong to the structural class of arylethanolamines (AEAs). The linkage between the aryl moiety and the amino group in AEAs is shorter than the AOPAs by an $-OCH_2-$ linkage [50]. In our docking studies, the AEAs are unable to interact with $Asn^{352\ (7.39)}$ while also maintaining the

group of $Leu^{65\ (1.39)}$ in tm1. (B) A 90° view of the aromatic cluster shown in (A). Both $Trp^{134\ (3.28)}$ and $Trp^{353\ (7.40)}$ lie above $Tyr^{356\ (7.43)}$. (C) Hydrogen bonding network involving $Ser^{190\ (4.57)}$, $Ser^{186\ (4.53)}$ and $Thr^{143\ (3.37)}$. The S190A mutation destroys the hydrogen bonds connecting $Ser^{190\ (4.57)}$ to $Ser^{186\ (4.53)}$ and $Thr^{143\ (3.37)}$. Distances shown are in angstroms (Å). Hydrogen atoms are not displayed.

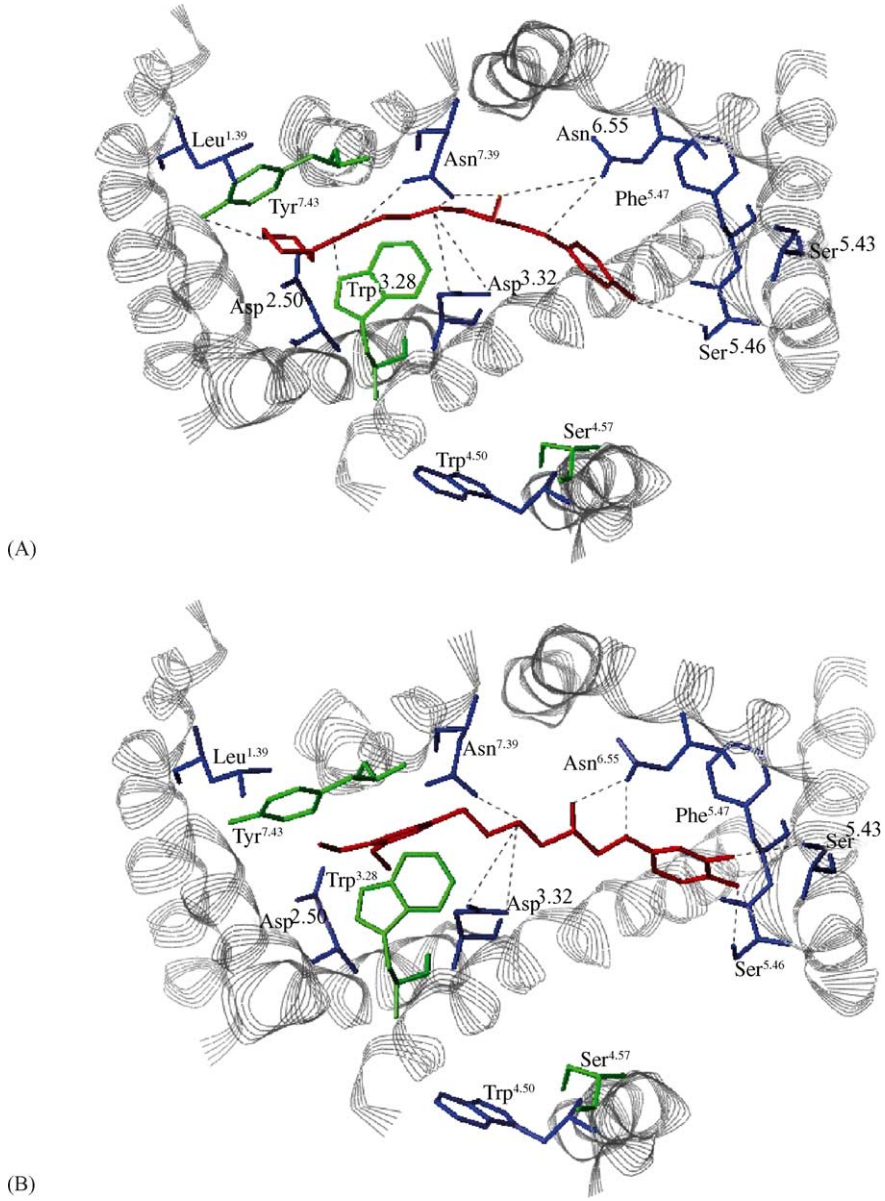

Fig. 6. Model of the 7tm regions of the WT rat β_1-AR with (A) *S*-xamoterol and (B) *S*-(−)-RO363 binding in an extended conformation. The colour scheme and representations are the same as for Fig. 3. A similar binding mode for *S*-(−)-RO363 in the human β_1-AR has also been described by Sugimoto et al. [37].

interactions with the Ser residues on tm5 and Asn$^{333\ (6.55)}$ on tm6 (Fig. 3A and B). This observation is consistent with the previous report [51] that the equivalent Asn residue in the β_2-AR (Asn$^{312\ (7.39)}$) is important for AOPA-type antagonist (alprenolol, pindolol, propanolol) binding but not for either AEA-type agonist ((−)-epinephrine, (−)-isoprenaline) or AEA-type antagonist (labetolol and sotalol) binding.

4. Discussion

One of the objectives of the study was to examine whether an interaction between Trp$^{134\ (3.28)}$ and Tyr$^{356\ (7.43)}$ restrains receptor activation in the β_1-AR. In bovine rhodopsin, the equivalent residues to Trp$^{134\ (3.28)}$ and Tyr$^{356\ (7.43)}$ form a salt bridge and breaking this restraint in rhodopsin leads to activation of the receptor

Fig. 7. Superimposition of *S*-xamoterol (black) and *S*-D150 (grey) in extended conformations illustrating the difference in ring conformations and the positions of the ring oxygen atoms.

[2,12]. In our studies, $Trp^{134\ (3.28)}$ and $Tyr^{356\ (7.43)}$ do not form a salt bridge (Fig. 3A), but are able to interact with each other via π–π interactions or a hydrogen bond when the Tyr side chain is rotated towards tm3. However, mutation of each of these two residues did not significantly change basal adenylyl cyclase activity or result in any of the other characteristics associated with constitutively active mutants such as increased agonist affinity or increased agonist dependent activity [4,7–9,46,47,52]. In fact, mutation of these residues resulted in a large drop in IA (53–88%) for (−)-isoprenaline and (46–61%) for (−)-RO363 compared to WT (Table 2). Hence, these residues, unlike the equivalent residues in GPCR opsin receptors, do not appear to play a role in maintaining the β_1-AR in the inactive state.

The most striking result, in this study, was that all three mutations (W134A, S190A and Y356F) significantly reduced adenylyl cyclase activation independently of their effects on agonist binding, even though β_1-AR expression (B_{max}) was not significantly different to the WT for all three mutant receptors ($P = 0.141$, Tables 1 and 2). In trying to explain our results, we noted that $Trp^{134\ (3.28)}$ and $Tyr^{356\ (7.43)}$, together with $Trp^{353\ (7.40)}$, in the rat β_1-AR are able to interact via π–π interactions to stabilize the extracellular ends of tms 3 and 7 (Fig. 5A and B). The interaction network between $Trp^{134\ (3.28)}$, $Trp^{353\ (7.40)}$ and $Tyr^{356\ (7.43)}$ would help to maintain the proper packing of the extracellular ends of tms 3 and 7 within the helix bundle. Our results demonstrate that single mutation of either $Trp^{134\ (3.28)}$ or $Tyr^{356\ (7.43)}$ results in substantial and equal reductions in IA and similar reductions in pD_2 (Table 2). If this site is important in the rotation of tms 3 and 7 during receptor activation, then mutation of these residues not only disrupts the orientation of the extracellular ends of tms 3 and 7 with respect to each other but would also disrupt the concerted movement of all tms during receptor activation. Maintenance of this cluster of aromatic residues appears to be essential for activation of the β_1-AR. They may play a similar role in the other mammalian amine GPCRs, since aromatic residues (Phe, Tyr and Trp) occur at residue position 3.28 in all of them, except for dopamine D_4 receptors where the residue is $Leu^{(3.28)}$, 5-HT_4Rs where it is $Arg^{(3.28)}$ and trace amine receptors which have $His^{(3.28)}$. At residue position 7.40, Trp is conserved and at residue position 7.43 it is either a Tyr or Trp (GPCRDB sequence alignment, February 2004 release 8.0, available at www.gpcr.org/7tm/). A large decrease in receptor activation has been reported for mutation of the analogous $Tyr^{(7.43)}$ residue in the angiotensin II_{1A} receptor [53] and in the 5-HT_{2A}R [54], which like the results presented here, cannot be explained by the small reduction in agonist-binding affinity seen in those studies.

The results for the mutation of $Ser^{190\ (4.57)}$ confirm a role for tm4 in the activation of the β_1-AR and suggest that the hydrogen bond network between $Ser^{190\ (4.57)}$, $Thr^{143\ (3.37)}$ and $Ser^{186\ (4.53)}$ is important in maintaining the spatial relationship between tms 3 and 4 (Fig. 5C). The S190A mutation removes two out of three hydrogen bond interactions in this region and reduces the IA by 53% and 46% and the pD_2 by 100- and 2000-fold for (−)-isoprenaline and (−)-RO363, respectively when compared to WT (Table 2). The disruption of the interhelical hydrogen bond network between tms 3 and 4 seems to be sufficient to interfere with the tm movement required for activation. Apart from the α_{1D}- and α_{2B}-ARs where residue position 4.53 is an Ala; $Ser^{(4.53)}$, $Thr^{(3.37)}$ and $Ser^{(4.57)}$are conserved across the mammalian adrenergic receptors and it is highly likely that they would play a similar role to that proposed here for the rat β_1-AR. The involvement of $Ser^{190\ (4.57)}$ in β_1-AR activation is also consistent with results for the H_4, where the analogous residue $Asn^{147\ (4.57)}$ affects receptor activation [27].

Our results also demonstrate that the mutant receptors had small effects on ligand binding (pK_i) in contrast to the large effect on IA. The exception was the large fall in pK_i for xamoterol at Y356F mutant receptors. The pK_i results for xamoterol support the hypothesis that $Tyr^{356\ (7.43)}$ interacts with the long amine substituent of large agonists and antagonists [20,21]. The loss in binding affinity observed for the Y356F mutant was much greater (126-fold) than that for all the other agonists studied (<20-fold, Table 1) and suggests a direct interaction between xamoterol and $Tyr^{356\ (7.43)}$. Unlike the other agonists examined, xamoterol not only has a long amine substituent which is able to bind deeply in the hydrophobic pocket located between tms 1, 2, 3 and 7 (defined by the residues $Leu^{65\ (1.39)}$, $Met^{107\ (2.53)}$, $Val^{111\ (2.57)}$, $Val^{112\ (2.58)}$, $Trp^{134\ (3.28)}$, $Asn^{352\ (7.39)}$, $Trp^{353\ (7.40)}$ and $Tyr^{356\ (7.43)}$) but also has an oxygen atom on the morpholino ring, which is able to hydrogen bond with the hydroxyl group of $Tyr^{356\ (7.43)}$ (Fig. 6A). Replacing $Tyr^{356\ (7.43)}$ with Phe maintains the aromatic bulk of the residue side chain but the ability to hydrogen bond is lost and this is the most likely explanation for the 126-fold loss in binding affinity. D150 has a similar structure to xamoterol (Fig. 1), but contains a tetrahydropyran ring, which adopts a slightly different conformation to the xamoterol morpholino ring (Fig. 7). As a result, D150 only binds at the entrance of the hydrophobic pocket and is not able to directly interact with $Tyr^{356\ (7.43)}$ if the interactions with the Ser residues on tm5 and $Asn^{333\ (6.55)}$ are maintained. This is reflected in the lower affinity of *S*-D150 in the WT and the smaller effect of the Y356F mutation on D150 binding compared to xamoterol (12-fold versus 126-fold, respectively, Table 1).

In contrast, mutation of $Trp^{134\ (3.28)}$ to Ala only had a small effect on xamoterol binding (8-fold) and did not adversely affect binding of *S*-(−)-RO363 or *S*-D150 (Table 1). The side chain of $Trp^{134\ (3.28)}$ provides a steric barrier for the bulky dimethoxyphenyl substituent of *S*-(−)-RO363 and the tetrahydropyran ring of *S*-D150 in the WT receptor (Fig. 6B), preventing the agonist amine

substituent from freely moving up towards the extracellular surface of the receptor. When minimizing the *S*-(−)-RO363 (or *S*-D150)–W134A receptor complex it was found that the *S*-(−)-RO363 dimethoxyphenyl ring had moved into the extra space created by the Trp to Ala mutation, enabling *S*-(−)-RO363 and *S*-D150 to adopt a less restricted conformation (docking results for the mutant receptor not shown here). This would explain the affinity for these two compounds being maintained at WT levels (Table 1).

For the S190A mutation, ∼10-fold reduction in binding affinity was observed for all of the agonists tested, with the exception of D150 (Table 1). Disruption of the hydrogen bond network around $Ser^{190\ (4.57)}$ (Fig. 5C) may weaken the interhelical interactions between tms 3 and 4 and allow movement of these tms. This may give the tetrahydropyran ring of *S*-D150 more room to bind thereby preserving its binding affinity at WT levels (Table 1) and at the same time reduce its ability to activate the receptor.

5. Conclusion

Our results suggest that interactions between $Trp^{134\ (3.28)}$, $Tyr^{356\ (7.43)}$ and $Trp^{353\ (7.40)}$ in the β_1-AR do not constrain the receptor in the inactivated state. Rather, this cluster of aromatic residues appears to be involved in maintaining the proper orientation of the extracellular ends of tms 3 and 7 within the helix bundle to allow the concerted movement of the tms during receptor activation. In addition, we argue that the hydrogen bond network between $Ser^{190\ (4.57)}$, $Thr^{143\ (3.37)}$ and $Ser^{186\ (4.53)}$ is important in maintaining the spatial relationship between tms 3 and 4 during β_1-AR activation. Our binding results are also consistent with an interaction between the amine substituent of xamoterol and $Tyr^{356\ (7.43)}$.

Acknowledgments

We thank Mr. David Casley for iodinating cyanopindolol, Ms. Heddy Wilshire for excellent technical assistance and Dr. Ian Gordon from the Statistical Consulting Centre at The University of Melbourne for assistance with the statistical analysis. This work was supported through grants from the Austin Hospital Medical Research Foundation and the C. Edward Dunlop Foundation. Simon N.S. Louis is supported by a National Health and Medical Research Council of Australia, INSERM Fellowship.

References

[1] Gether U. Uncovering molecular mechanisms involved in activation of G protein-coupled receptors. Endo Rev 2000;21:90–113.

[2] Filipek S, Teller DC, Palczewski K, Stenkamp R. The crystallographic model of rhodopsin and its use in studies of other G protein-coupled receptors. Annu Rev Biophys Biomol Struct 2003;32:375–97.

[3] Miura S, Zhang J, Boros J, Karnik SS. TM2-TM7 interaction in coupling movement of transmembrane helices to activation of the angiotensin II type-1 receptor. J Biol Chem 2003;278:3720–5.

[4] Hannawacker A, Krasel C, Lohse MJ. Mutation of Asn293 to Asp in transmembrane helix VI abolishes agonist-induced but not constitutive activity of the β_2-adrenergic receptor. Mol Pharmacol 2002;62:1431–7.

[5] Chen S, Lin F, Xu M, Graham RM. Phe^{303} in TMVI of the α_{1B}-adrenergic receptor is a key residue coupling TM helical movements to G-protein activation. Biochemistry 2002;41:588–96.

[6] Yeagle PL, Albert AD. A conformational trigger for activation of a G protein by a G protein-coupled receptor. Biochemistry 2003;42:1365–8.

[7] Hunyady L, Vauquelin G, Vanderheyden P. Agonist induction and conformational selection during activation of a G-protein-coupled receptor. Trends Pharm Sci 2003;24:81–6.

[8] Karnik SS, Gogonea C, Patil S, Saad Y, Takezako T. Activation of G-protein-coupled receptors: a common molecular mechanism. Trends Endo Metab 2003;14:431–7.

[9] Decaillot FM, Befort K, Filliol D, Yue SY, Walker P, Kieffer BL. Opioid receptor random mutagenesis reveals a mechanism for G protein-coupled receptor activation. Nat Struct Biol 2003;10:629–36.

[10] Swaminath G, Xiang Y, Lee TW, Steenhuis J, Parnot C, Kobilka BK. Sequential binding of agonists to the β_2-adrenoceptor. Kinetic evidence for intermediate conformational states. J Biol Chem 2004;279:686–91.

[11] Chen S, Lin F, Xu M, Riek P, Novotny J, Graham RM. Mutation of a single TMV1 residue, Phe^{282}, in the β_2-adrenergic receptor results in structurally distinct activated receptor conformations. Biochemistry 2002;41:6045–53.

[12] Palczewski K, Kumasaka T, Hori T, Behnke CA, Motoshima H, Fox BA, et al. Crystal structure of rhodopsin: a G protein-coupled receptor. Science 2000;289:739–45.

[13] Befort K, Zilliox C, Filliol D, Yue SY, Kieffer BL. Constitutive activation of the δ opioid receptor by mutations in transmembrane domains III and VII. J Biol Chem 1999;274:18574–81.

[14] Porter EJ, Hwai J, Perez DM. Activation of the α_{1b}-adrenergic receptor is initiated by disruption of an interhelical salt bridge contraint. J Biol Chem 1996;271:28318–23.

[15] Berthold K, Louis WJ, Stoll A. 3-Aminopropoxyphenyl derivatives, their preparation and pharmaceutical compositions containing them. 1987 USA Patent No. 4661513.

[16] Iakovidis D, Louis SNS, Rezmann LA, Colagrande F, Nero TL, Jackman GP, et al. Synthesis and β-adrenoceptor agonist properties of (±)-1-(3′,4′-dihydroxyphenoxy)-3-(3″,4″-dimethoxyphenyl)ethylamino-2-propanol hydrochloride, (±)-RO363.HCl, and the (2*S*)-(−)-isomer. Eur J Med Chem 1999;34:539–48.

[17] Louis SN, Nero TL, Iakovidis D, Colagrande FM, Jackman GP, Louis WJ. β_1- and β_2-Adrenoceptor antagonist activity of a series of *para*-substituted *N*-isopropylphenoxypropanolamines. Eur J Med Chem 1999;34:919–37.

[18] Louis SN, Rezmann-Vitti LA, Nero TL, Iakovidis D, Jackman GP, Louis WJ. CoMFA analysis of the human β_1-adrenoceptor binding affinity of a series of phenoxypropanolamines. Eur J Med Chem 2002;37:111–25.

[19] Jackman GP, Iakovidis D, Nero TL, Anavekar NS, Rezmann-Vitti LA, Louis SNS, et al. Synthesis, β-adrenoceptor pharmacology and toxicology of *S*-(−)-1-(4-(2-ethoxyethoxy)phenoxy)-2-hydroxy-3-(2-(3,4-dimethoxyphenyl)ethylamino)propane hydrochloride, a short acting β_1-specific antagonist. Eur J Med Chem 2002;37:731–41.

[20] Nero TL, Iakovidis D, Louis WJ. Molecular modeling of the human β_1-adrenoceptor. In: Sanz F, Giraldo J, Manaut F, editors. QSAR and molecular modeling: concepts, computational tools and biological

applications. Barcelona: Prous Science Publishers; 1995. p. 528–30.
[21] Louis SNS. Ligand–receptor interactions at beta-adrenoceptors in mammalian tissues. PhD thesis. Victoria: The University of Melbourne; 1997.
[22] Furse KE, Lybrand TP. Three-dimensional models for β-adrenergic receptor complexes with agonists and antagonists. J Med Chem 2003;46:4450–62.
[23] Dixon RAF, Sigal IS, Strader CD. Structure–function analysis of the β-adrenergic receptor. Cold Spring Harbor Symp Quant Biol 1988;3:487–97.
[24] Unger VM, Hargrave PA, Baldwin JM, Schertler GF. Arrangement of rhodopsin transmembrane-helices. Nature 1997;389:203–6.
[25] Lu ZL, Saldanha JW, Hulme EC. Transmembrane domains 4 and 7 of the M_1 muscarinic acetylcholine receptor are critical for ligand binding and the receptor activation switch. J Biol Chem 2001;276:34098–104.
[26] Jakubik J, El-Fakahany EE, Tucek S. Evidence for a two-site model of ligand binding to muscarinic acetylchloline receptors. J Biol Chem 2001;275:18836–44.
[27] Shin N, Coates E, Murgolo NJ, Morse KL, Bayne M, Strader CD, et al. Molecular modeling and site-specific mutagenesis of the histamine-binding site of the histamine H_4 receptor. Mol Pharmacol 2002; 62:38–47.
[28] Manivet P, Schnieder B, Smith JC, Choi D, Maroteaux L, Kellerman O, et al. The serotonin binding site of human and murine 5-HT_{2B} receptors. Molecular modeling and site-directed mutagenesis. J Biol Chem 2002;277:17170–8.
[29] Strosberg AD, Camoin L, Blin N, Maigret B. In receptors coupled to GTP-proteins, ligand binding and G-protein activation is a multistep dynamic process. Drug Des Discov 1993;9:199–211.
[30] Lew R, Summers RJ. Autoradiographic localisation of β-adrenoceptor subtypes in guinea-pig kidney. Br J Pharmacol 1985;85:341–8.
[31] Blin N, Camoin L, Maigret B, Strosberg AD. Structural and conformational features determining selective signal transduction in the β_3-adrenergic receptor. Mol Pharmacol 1993;44:1094–104.
[32] Bradford MM. A rapid and sensitive method for the quantitation of microgram quantities of protein utilizing the principle of protein-dye binding. Anal Biochem 1976;72:248–54.
[33] Munson PJ, Rodbard D. LIGAND: a versatile computerised approach for the characterisation of ligand binding systems. Anal Biochem 1980;109:220–39.
[34] McPherson GA. A practical computer-based approach to the analysis of radioligand binding experiments. Comput Programs Biomed 1983;17:107–13.
[35] Cox DR. Analysis of binary data. London: Chapman and Hall; 1970. p. 33.
[36] Ballesteros JA, Weinstein H. Integrated methods for the construction of three-dimensional models and computational probing of structure-function relations in G protein-coupled receptors. Methods Neurosci 1995;25:366–428.
[37] Sugimoto Y, Fujisawa R, Tanimura R, Lattion AL, Cotecchia S, Tsujimoto G, et al. β_1-Selective agonist (−)-1-(3,4-dimethoxyphenethylamino)-3-(3,4-dihydroxy)-2-propanol [(−)-RO363] differentially interacts with key amino acids responsible for β_1-selective binding in resting and active states. J Pharmacol Exp Therap 2002;301:51–8.
[38] Strader CD, Candalore MR, Hill WS, Dixon RAF, Sigal IS. Identification of two serine residues involved in agonist activation of the β-adrenergic receptor. J Biol Chem 1989;264:13572–8.
[39] Liapakis G, Ballesteros JA, Papachristou S, Chan WC, Chen X, Javitch JA. The forgotten serine: a critical role for Ser203 in ligand binding to and activation of the β_2-adrenergic receptor. J Biol Chem 2000;275:37779–88.
[40] Del Carmine R, Ambrosio C, Sbraccia M, Cotecchia S, Ijzerman AP, Costa T. Mutations inducing divergent shifts of constitutive activity reveal different modes of binding among catecholamine analogues to the β_2-adrenergic receptor. Br J Pharmacol 2002;135: 1715–22.
[41] Wieland K, Zuurmond HM, Krasel C, Ijzerman AP, Lohse MJ. Involvement of Asn-293 in stereospecific agonist recognition and in activation of the beta 2-adrenergic receptor. Proc Natl Acad Sci USA 1996;93:9276–81.
[42] Lewell XQ. A model of the adrenergic beta-2 receptor and binding sites for agonist and antagonist. Drug Des Discov 1992;9: 29–48.
[43] Trumpp-Kallmeyer S, Hoflack J, Bruinvels A, Hibert M. Modeling of G-protein-coupled receptors: application to dopamine, adrenaline, serotonin, acetylcholine, and mammalian opsin receptors. J Med Chem 1992;35:3448–62.
[44] Vaidehi N, Floriano WB, Trabanino R, Hall SE, Freddolino P, Choi EJ, et al. Prediction of structure and function of G protein-coupled receptors. Proc Natl Acad Sci USA 2002;99:12622–7.
[45] Freddolino PL, Kalani MYS, Vaidehi N, Floriano WB, Hall SE, Trabanino RJ, et al. Predicted 3D structure for the β_2 adrenergic receptor and its binding site for agonists and antagonists. Proc Natl Acad Sci USA 2004;101:2736–41.
[46] Greasley PJ, Fanelli F, Rossier O, Abuin L, Cotecchia S. Mutagenesis and modelling of the α_{1b}-adrenergic receptor highlight the role of the helix 3/helix 6 interface in receptor activation. Mol Pharmacol 2002;61:1025–32.
[47] Mclean AJ, Zeng F, Behan D, Chalmers D, Milligan G. Generation and analysis of constitutively active and physically destabilized mutants of the human β_1-adrenoceptor. Mol Pharmacol 2002;62:747–55.
[48] Shi L, Liapakis G, Xu R, Guarnieri F, Ballesteros JA, Javitch JA. β_2 adrenergic receptor activation. Modulation of the proline kink in transmembrane 6 by a rotamer toggle switch. J Biol Chem 2002;277:40989–96.
[49] Gabilondo AM, Krasel C, Lohse MJ. Mutations of Tyr^{326} in the beta 2-adrenoceptor disrupt multiple receptor functions. Eur J Pharmacol 1996;307:243–50.
[50] Nero TL, Louis WJ, Iakovidis D. β-Adrenoceptor agonists and antagonists: conformational analysis of the ethanolamine and propanolamine side-chain. J Mol Struct 1993;285:251–72.
[51] Suryanarayana S, Kobilka BK. Amino acid substitutions at position 312 in the seventh hydrophobic segment of the β_2-adrenergic receptor modify ligand-binding specificity. Mol Pharmacol 1993; 44:111–4.
[52] Pei G, Samama P, Loshe M, Wang M, Codina J, Lefkowitz RJ. A constitutively active mutant β_2-adrenergic receptor is constitutively densensitizied and phosphorylated. Proc Natl Acad Sci USA 1994;91:2699–702.
[53] Marie J, Maigret B, Joseph MP, Larguier R, Nouet S, Lombard C, et al. Tyr^{292} in the seventh transmembrane domain of the AT1A angiotensin II receptor is essential for its coupling to phospholipase C. J Biol Chem 1994;33:20815–8.
[54] Roth BL, Shoham M, Choudhary MS, Khan N. Identification of conserved aromatic residues essential for agonist binding and second messenger production at 5-hydroxytryptamine$_{2A}$ receptors. Mol Pharmacol 1997;52:259–66.